END

FILMED

MICROCOPY RESOLUTION TEST CHART
NATIONAL BUREAU OF STANDARDS-1963-A

A134 055

(12)

DAVID W. TAYLOR NAVAL SHIP
RESEARCH AND DEVELOPMENT CENTER

Bethesda, Maryland 20C84

IMPROVED PREDICTION OF DRIFT FORCES AND MOMENT

by

Young S. Hong

DTIC
ELECTE
OCT 2 6 1983

B

SHIP PERFORMANCE DEPARTMENT
RESEARCH AND DEVELOPMENT REPORT

September 1983   DTNSRDC-83/069

83 10 25 046

MAJOR DTNSRDC ORGANIZATIONAL COMPONENTS

```
                        ┌─────────────────────┐
                        │      DTNSRDC         │
                        │     COMMANDER    00  │
                        │  TECHNICAL DIRECTOR  │
                        │                  01  │
                        └─────────────────────┘

┌─────────────────────┐               ┌─────────────────────┐
│ OFFICER-IN-CHARGE    │               │ OFFICER-IN-CHARGE    │
│ CARDEROCK        05  │               │ ANNAPOLIS        04  │
└─────────────────────┘               └─────────────────────┘

┌─────────────────────┐
│ SYSTEMS              │
│ DEVELOPMENT          │
│ DEPARTMENT       11  │
└─────────────────────┘

┌─────────────────────┐               ┌─────────────────────┐
│ SHIP PERFORMANCE     │               │ AVIATION AND         │
│ DEPARTMENT           │               │ SURFACE EFFECTS      │
│                  15  │               │ DEPARTMENT       16  │
└─────────────────────┘               └─────────────────────┘

┌─────────────────────┐               ┌─────────────────────┐
│ STRUCTURES           │               │ COMPUTATION,         │
│ DEPARTMENT           │               │ MATHEMATICS AND      │
│                  17  │               │ LOGISTICS DEPARTMENT │
│                      │               │                  18  │
└─────────────────────┘               └─────────────────────┘

┌─────────────────────┐               ┌─────────────────────┐
│ SHIP ACOUSTICS       │               │ PROPULSION AND       │
│ DEPARTMENT           │               │ AUXILIARY SYSTEMS    │
│                  19  │               │ DEPARTMENT       27  │
└─────────────────────┘               └─────────────────────┘

┌─────────────────────┐               ┌─────────────────────┐
│ SHIP MATERIALS       │               │ CENTRAL              │
│ ENGINEERING          │               │ INSTRUMENTATION      │
│ DEPARTMENT       28  │               │ DEPARTMENT       29  │
└─────────────────────┘               └─────────────────────┘
```
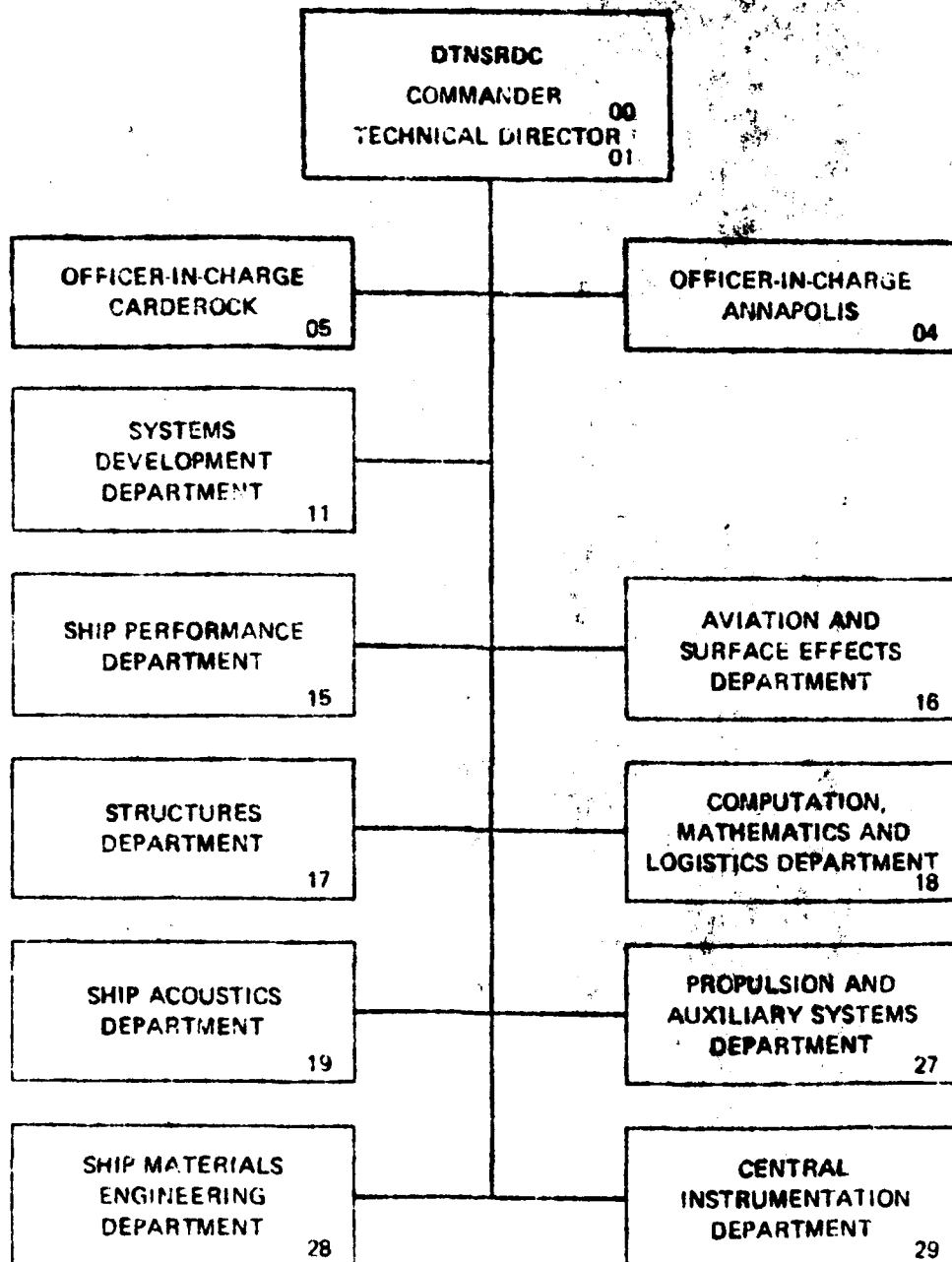
REPORT DOCUMENTATION PAGE	READ INSTRUCTIONS BEFORE COMPLETING FORM
1. REPORT NUMBER DTNSRDC-83/069 2. GOVT ACCESSION NO. *AI34050*	3. RECIPIENT'S CATALOG NUMBER
4. TITLE (and Subtitle) IMPROVED PREDICTION OF DRIFT FORCES AND MOMENT	5. TYPE OF REPORT & PERIOD COVERED Final
	6. PERFORMING ORG. REPORT NUMBER
7. AUTHOR(s) Young S. Hong	8. CONTRACT OR GRANT NUMBER(s)
9. PERFORMING ORGANIZATION NAME AND ADDRESS David W. Taylor Naval Ship Research and Development Center Bethesda, Maryland 20084	10. PROGRAM ELEMENT, PROJECT, TASK AREA & WORK UNIT NUMBERS (See reverse side)
11. CONTROLLING OFFICE NAME AND ADDRESS	12. REPORT DATE September 1983
	13. NUMBER OF PAGES 42
14. MONITORING AGENCY NAME & ADDRESS(if different from Controlling Office)	15. SECURITY CLASS. (of this report) UNCLASSIFIED
	15a. DECLASSIFICATION/DOWNGRADING SCHEDULE

16. DISTRIBUTION STATEMENT (of this Report)

APPROVED FOR PUBLIC RELEASE: DISTRIBUTION UNLIMITED

17. DISTRIBUTION STATEMENT (of the abstract entered in Block 20, if different from Report)

18. SUPPLEMENTARY NOTES

19. KEY WORDS (Continue on reverse side if necessary and identify by block number)

20. ABSTRACT (Continue on reverse side if necessary and identify by block number)

A three-dimensional method is developed to improve the computation of the drift force and moment for small-waterplane-area, twin-hull (SWATH) and surface ships in oblique waves with zero forward speed. Numerical results have been computed for three ships: SWATH 6A, Stretched SSP, and MCM 5371. The results for Stretched SSP show good agreement with experiment. For MCM 5371, the results of two- and three-dimensional methods are

(Continued on reverse side)

(Block 10)

Program Element 61153N
Task Area SR0230101
Work Unit 1562-201

(Block 20 continued)

almost identical to each other and these results show good agreement
with experiment when the wavelength ratio is not too small. Even
though there are no test data available for SWATH 6A, the application
of three-dimensional theory is likely to improve the results of drift
force and moment for SWATH ships.

DTIC
S ELECTE D
OCT 26 1983

B

Accession For

NTIS GRA&I	✓	
DTIC TAB	☐	
Unannounced	☐	
Justification		

By
Distribution/

Availability Codes

Dist	Avail and/or Special
A	

TABLE OF CONTENTS

LIST OF FIGURES

NOTATION

A	Amplitude of incoming wave
F_x, F_y, M_z	Horizontal forces and their moment with respect to the z-axis
$\bar{F}_x$, $\bar{F}_y$, $\bar{M}_z$	Drift forces and yaw moment
G	Green function
g	Gravitational acceleration
$H(\theta)$	Kochin function
Im	Imaginary part of a complex value
$i = (-1)^{1/2}$	Imaginary unit
J_o	Bessel function of the first kind
$K = \omega^2/g$	Incoming wave number
L	Characteristic ship's length
$n_j = (n_x, n_y, n_z)$	Unit normal vector directed into the fluid
p	Pressure
$Q_j (j=1,2, \ldots ,7)$	Source density
R	$(x^2+y^2)^{1/2}$
Re	Real part of a complex value
R_1	$((x-x')^2+(y-y')^2+(z-z')^2)^{1/2}$
R_2	$((x-x')^2+(y-y')^2+(z+z')^2)^{1/2}$
r	$((x-x')^2+(y-y')^2)^{1/2}$
S_B	Wetted body surface

S_F	Free Surface
S_∞	Control surface at infinity
TA	Time average
$\vec{U} = (U_x, U_y, U_z)$	Flow velocity at the body surface
$\vec{V} = (V_x, V_y, V_z)$	Flow velocity
ζ	Free-surface wave height
λ	Incoming wave length
$\xi_j (j=1,2, \ldots ,6)$	Amplitude of motion in each of six degrees of freedom (surge, sway, heave, roll, pitch, and yaw)
ρ	Water density
ϕ_B	Disturbed velocity potential due to the presence of the ship
ϕ_I	Incoming wave potential
φ_7	Diffraction potential
$\varphi_j (j=1,2, \ldots ,6)$	Velocity potential due to motion of ship with unit amplitude in each of six degrees of freedom
ω	Incoming wave frequency

ABSTRACT

A three-dimensional method is developed to improve the computation of the drift force and moment for small-waterplane-area, twin-hull (SWATH) and surface ships in oblique waves with zero forward speed. Numerical results have been computed for three ships: SWATH 6A, Stretched SSP, and MCM 5371. The results for Stretched SSP show good agreement with experiment. For MCM 5371, the results of two- and three-dimensional methods are almost identical to each other and these results show good agreement with experiment when the wavelength ratio is not too small. Even though there are no test data available for SWATH 6A, the application of three-dimensional theory is likely to improve the results of drift force and moment for SWATH ships.

ADMINISTRATIVE INFORMATION

INTRODUCTION

The study of steady and slowly varying forces and moments on a ship in oblique waves is important to maneuvering and seakeeping analyses, particularly when mission requirements include station keeping or very low speed maneuvering. Recent examples of Navy ship designs which include such requirements are T-AGOS (a small-waterplane-area, twin-hull or SWATH ship) and a monohull mine countermeasures (MCM) ship.

Maruo[1]* has derived the equations for drift forces in terms of scattered wave amplitudes for the two-dimensional problem and in terms of a Kochin function for the three-dimensional problem. However, he has provided no numerical computation of his analytic results. Newman[2] has derived the equations for drift forces and yaw moment for the three-dimensional problem using a slender body assumption and computed forces and moment for a Series 60, $C_B = 0.6$, Lee and Kim[3] have recently derived the equation for the roll moment in addition to drift forces and yaw moment and computed forces and moments for a SWATH ship and a monohull ship through a two-dimensional motion program.

---

*A complete listing of references is given on page 23.

The present study consists of the application of three-dimensional motion results to linear theory. The force and moment equations are derived with application of the rate of change of linear momentum and angular momentum previously presented by Newman.[2] The disturbance velocity potential is computed with the three-dimensional motion program for zero forward speed developed by Hong and Paulling.[4] For numerical computation of drift forces and yaw moment, three models have been selected: SWATH 6A, Stretched SSP, and MCM 5371. The results for Stretched SSP show good agreement with experiment. For MCM 5371, the results of two- and three-dimensional methods are almost identical to each other, and these results show good agreement with experiment when the wavelength ratio is not too small. Even though there are no test data available for SWATH 6A, the application of three-dimensional theory is likely to improve the results of drift force and moment for SWATH ships.

THREE-DIMENSIONAL SOLUTION OF THE VELOCITY POTENTIAL

The coordinate system, oxyz, is defined to be fixed to the ship with no forward speed. The oz-axis is directed vertically upward, and the ox-axis is positive towards the bow. The oxy-plane is the undisturbed free surface. It is assumed that the fluid is incompressible and inviscid, and the flow is irrotational. The total velocity potential of the fluid in incoming waves in the presence of the ship is represented by

$$\Phi(x,y,z,t) = Re[\phi(x,y,z)e^{-i\omega t}] = Re[(\phi_I+\phi_B)e^{-i\omega t}] \tag{1}$$

where ϕ_I is the potential of the incoming wave and is given by

$$\phi_I = -\frac{igA}{\omega} \exp[Kz+iKx \cos \beta - iKy \sin \beta] \tag{2}$$

and ϕ_B is the disturbance velocity potential due to the presence of the ship. In Equation (2), A is the amplitude of the incoming wave, ω is its frequency, g is the gravitational acceleration, β is the angle of incoming wave relative to the x-axis ($\beta = 0$, following sea and 180, head sea), and $K = \omega^2/g$ is the wave number. The potential consists of the following velocity potentials as

2

$$\phi_B = \varphi_7 + \sum_{j=1}^{6} \xi_j \varphi_j \tag{3}$$

where φ_j (j=1,2,...,6) is the velocity potential arising from the motion of ship with unit amplitude in each of six degrees of freedom, and ξ_j (j=1,2,...,6) is the amplitude of motion in each of six degrees of freedom. The diffraction potential is represented by φ_7.

The potential φ_j is determined as the solution of the following conditions:

1. Laplace equation in the fluid domain

$$\frac{\partial^2 \varphi_j}{\partial x^2} + \frac{\partial^2 \varphi_j}{\partial y^2} + \frac{\partial^2 \varphi_j}{\partial z^2} = 0, \qquad \text{for } j=1,2,\ldots,7 \tag{4}$$

2. the body boundary condition

$$\frac{\partial \varphi_j}{\partial n} = -i \omega n_j, \qquad \text{for } j=1,2,\ldots,6 \tag{5}$$

$$\frac{\partial \varphi_j}{\partial n} = -\frac{\partial \phi_I}{\partial n}, \qquad \text{for } j=7 \tag{6}$$

3. the linearized free-surface condition

$$K \varphi_j - \frac{\partial \varphi_j}{\partial z} = 0 \qquad \text{on } z=0 \tag{7}$$

The right-hand side of Equation (5) is the normal velocity component at the ship's surface and the unit normal vector is directed into the fluid domain. In addition to Equations (5) through (7), φ_j must satisfy the radiation condition of outgoing waves at infinity and become zero as z becomes infinitely negative.

The solution of Equation (4) with the boundary conditions, Equations (5) through (7), has been presented by Hong and Paulling[4] in terms of Green's function as:

3

$$\varphi_j = \iint\limits_{S_B} Q_j(x',y',z')\, G(x,y,z;x',y',z')\, dS \qquad (8)$$

The integral in Equation (8) is evaluated over the average wetted surface of the body, S_B. The unknown source density is Q_j, and G is the Green function for the problem. The Green function for a pulsating source in deep water can be written as presented by Wehausen and Laitone[5] as:

$$G(x,y,z;x',y',z') = \frac{1}{R_1} + \frac{1}{R_2} + 2K \, pv \int_0^\infty \frac{e^{\mu(z+z')}}{\mu-K} \, J_o(\mu r) \, d\mu$$

$$+ \, i2\pi K \, e^{K(z+z')} \, J_o(Kr) \qquad (9)$$

where J_o is the Bessel function of the first kind of zero order and

$$R_1^2 = (x-x')^2 + (y-y')^2 + (z-z')^2 \qquad (10)$$

$$R_2^2 = (x-x')^2 + (y-y')^2 + (z+z')^2 \qquad (11)$$

$$r^2 = (x-x')^2 + (y-y')^2 \qquad (12)$$

The source density, Q_j can be found by applying the body boundary conditions. From Equations (5) and (6), the source density may be represented as:

$$-2\pi \, Q_j(x,y,z) + \frac{\partial}{\partial n} \iint\limits_{S_B} Q_j(x',y',z')\, G(x,y,z;x',y',z')\, dS$$

$$= -i \, \omega \, n_j, \qquad \text{for } j=1,2,\ldots,6 \qquad (13)$$

$$= -\frac{\partial \phi_I}{\partial n}, \qquad \text{for } j=7 \qquad (14)$$

The numerical solution of these equations is given in Reference 4.

EQUATIONS FOR DRIFT FORCES AND MOMENT

The surface which enclosed the fluid domain is divided into three subregions: S_B ship's wetted surface, S_F free surface and S control surface at infinity (see Figure 1). The rate of change of the linear and angular momentum is given by (Reference 1):

$$\frac{dM_x}{dt} = - \iint_{S_B+S_F+S_\infty} [pn_x + \rho V_x(V_n - U_n)] \, dS \qquad (15)$$

$$\frac{dM_y}{dt} = - \iint_{S_B+S_F+S_\infty} [pn_y + \rho V_y(V_n - U_n)] \, dS \qquad (16)$$

$$\frac{dK_z}{dt} = - \iint_{S_B+S_F+S_\infty} [p(xn_y - yn_x) + \rho(xV_y - yV_x)(V_n - U_n)] \, dS \qquad (17)$$

where p $\quad$ = fluid pressure

$\quad \rho \quad$ = density

$\quad (n_x, n_y, n_z)$ = components of the unit vector $\vec{n}$

$\quad U_n \quad$ = normal velocity on S_B, and

$\quad (V_x, V_y, V_z)$ = components of the velocity $\vec{V}$

On the body surface and free surface, $V_n = U_n$. The contribution from the pressure term on S_B is the vector of forces and moment acting on the body:
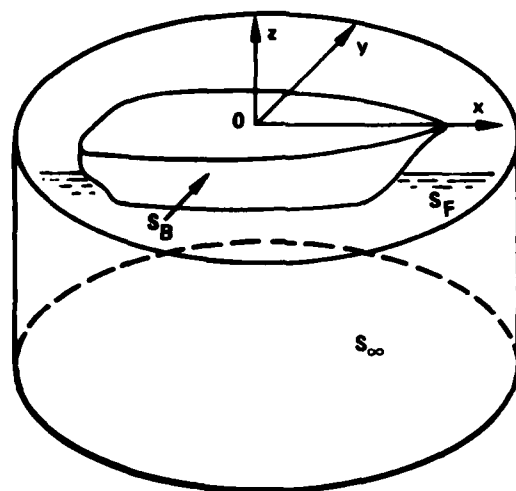
$$F_x = - \iint_{S_B} p \, n_x \, dS \qquad (18)$$

5

Figure 1 - Control Surface

$$F_y = - \iint_{S_B} p \, n_y \, dS \tag{19}$$

$$M_z = - \iint_{S_B} p(xn_y - yn_x) \, dS \tag{20}$$

With $U_n = 0$ on S and $p = 0$ on S_F, the forces and moment become as follows

$$F_x = \iint_{S_\infty} [pn_x + \rho V_x V_n] \, dS + \frac{dM_x}{dt} \tag{21}$$

$$F_y = \iint_{S_\infty} [pn_y + \rho V_y V_n] \, dS + \frac{dM_y}{dt} \tag{22}$$

$$M_z = \iint_{S_\infty} [p(xn_y - yn_x) + \rho(xV_y - yV_x)V_n] \, dS + \frac{dK_z}{dt} \tag{23}$$

6

The time averages of Equations (21), (22), and (23) are the mean drift forces and moment. Since the time average of linear momentum of the periodic motion is zero, the drift forces and moment are given as

$$\bar{F}_x = \overline{\iint_{S_\infty} [pn_x + \rho V_x V_n] \, dS} \tag{24}$$

$$\bar{F}_y = \overline{\iint_{S_\infty} [pn_y + \rho V_y V_n] \, dS} \tag{25}$$

$$\bar{M}_z = \overline{\iint_{S_\infty} [p(xn_y - yn_x) + \rho(xV_y - yV_x)V_n] \, dS} \tag{26}$$

The pressure in these equations is given by Bernoulli's equation

$$p = -\rho \, Re(-i\omega\phi e^{-i\omega t}) - \frac{1}{2}\rho|\vec{V}|^2 - \rho g z \tag{27}$$

The control surface S_∞ consists of a circular cylinder of large radius about the z-axis and extending from the free surface to $z = -\infty$. On S_∞, the boundary conditions are represented in cylindrical polar coordinates with $x = r \cos\theta$ and $y = r \sin\theta$. Through a substitution of the pressure terms and taking the time average of the velocity potential the drift forces and moment are given by

$$\bar{F}_x = -\frac{\rho K^2}{8\pi} \int_0^{2\pi} |H(\pi+\theta)|^2 \cos\theta \, d\theta + \frac{\rho\omega A}{2} \cos\beta \, Re[H(\pi-\beta)] \tag{28}$$

$$\bar{F}_y = -\frac{\rho K^2}{8\pi} \int_0^{2\pi} |H(\pi+\theta)|^2 \sin\theta \, d\theta - \frac{\rho\omega A}{2} \sin\beta \, Re[H(\pi-\beta)] \tag{29}$$

7

$$\bar{M}_z = -\frac{\rho K}{8\pi} \text{ Im} \int_0^{2\pi} H^*(\pi+\theta) \ H'(\pi+\theta) \ d\theta + \frac{\rho \omega A}{2K} \text{ Im}[H'(\pi-\beta)] \qquad (30)$$

The details of derivation are given in Reference 1 and in Appendix A. Here, $H(\theta)$ is the Kochin function and defined as

$$H(\theta) = -\iint_{S_B} \left(\frac{\partial \phi_B}{\partial n} - \phi_B \frac{\partial}{\partial n} \right) \exp(Kz + iKx \cos\theta + iKy \sin\theta) \ dS \qquad (31)$$

The asterisk (in Equation (30)) denotes the complex conjugate, the prime denotes the derivative with respect to θ, and Re and Im mean the real and imaginary parts of the complex value.

If we substitute Equation (3) for ϕ_B, the Kochin function can be written

$$H(\theta) = H_7(\theta) + \sum_{j=1}^{6} \xi_j \ H_j(\theta) \qquad (32)$$

where

$$H_j(\theta) = -\iint_{S_B} \left(\frac{\partial \varphi_j}{\partial n} - \varphi_j \frac{\partial}{\partial n} \right) \exp[Kz + iK(x \cos\theta + y \sin\theta)] \ dS \qquad (33)$$

The exciting forces can be expressed in terms of the Kochin function (see Appendix B) as

$$F_j = \frac{\rho g A}{\omega} \ [-\text{Im } H_j(-\beta) + i \text{ Re } H_j(-\beta)] \qquad (34)$$

Equation (34) is useful in order to check the numerical evaluation of Kochin functions by comparing with the motion results.

8

RESULTS AND DISCUSSIONS

In order to validate the numerical results of the derived equations, three hull forms have been selected: SWATH 6A, Stretched SSP, and MCM 5371. The last hull form is a surface ship. The principal parameter values of these three hull forms are given in Table 1.

TABLE 1 - VALUES OF PRINCIPAL PARAMETERS*

Parameter (and Unit)	SWATH 6A	Stretched SSP	MCM 5371
Displacement (long ton)	2579	618	1725
Characteristic Length L (m)	54.3	45.5	73.2
Length of Waterline (m)	52.5	42.4	--
Length of Main Hull (m)	73.2	46.3	--
Beam of Each Hull at Waterline (m)	2.2	3.4	13.4
Draft at Midship (m)	8.1	5.0	3.6
Maximum Diameter of Main Hull (m)	4.6	3.4	--
Hull Spacing (m)	22.9	12.2	--
Longitudinal Center of Gravity Aft of Main Hull Nose (m)	35.5	21.9	37.9
Longitudinal Center of Floatation Aft of Main Hull Nose (m)	35.2	24.6	41.4
Vertical Center of Gravity (m)	10.4	4.9	5.3
Longitudinal GM (m)	6.8	18.7	73.2
Transverse GM (m)	3.4	1.5	1.9
Radius of Gyration for Pitch (m)	17.1	12.4	18.3
Radius of Gyration for Roll (m)	12.1	5.6	5.3
Waterplane Area (m^2)	193.9	68.4	739.0
Length of Strut (m)	52.4	31.5	--
Strut Gap (m)	--	10.8	--
Maximum Strut Thickness (m)	2.2	1.2	--

*Dimensions are full scale.

9

The numerical results of SWATH 6A are shown in Figures 2-5. Figures 2 and 3 show the results of head sea; Figures 4 and 5 show the results of beam sea. At head sea, either motion results or results of sway drift force show good agreement between two- and three-dimensional results except for small λ/L values where the two-dimensional theory diverges from its asymtotic value. In beam waves, the results of sway drift force and yaw drift moment show some discrepancies between two- and three-dimensional approaches. Without the experimental results, it is impossible to judge which one is correct. These discrepancies occur even in the results of restrained motion (if this is the case, only the diffraction potential is included in the computation). This indicates that in the solution of the diffraction potential, the longitudinal interaction of the sections plays an important role. The strut length of SWATH 6A is 52.4 m and the length of the main hull is 73.2 m. Where the strut ends, one section is fully submerged and the other is floating in the two-dimensional model. The interaction of these two sections is not included in the two-dimensional approach; however, in the present method, this interaction is fully taken into account. The full effect of this interaction will be shown in a following example for the Stretched SSP. The two- and three-dimensional results for heave and pitch motions show good agreement with each other and these results for heave motion are in good agreement with test data. However, the analytical results for roll motion show large discrepancies from the test results. These discrepancies are probably due to the effect of fins since, in the analytical method, the effect of fins is not included in the motion results.

Figures 6-7 show the computational and experimental results for the Stretched SSP in beam waves. The computed sway forces here are compared with the experimental results presented by Numata.[8] There are some minor differences between the three-dimensional results and test results; however, the general trend is the same. The two-dimensional results show major differences. As shown in the motion results, especially for roll motion, the two-dimensional results show large discrepancies from the three-dimensional results and the test data. The agreement of roll motion between three-dimensional results and the test is very good; however, there are some discrepancies in heave motion when λ/L is larger than 1.5. These discrepancies do not affect the results for drift forces since, when λ/L is larger than 1.5, the sway drift forces become very small for the three-dimensional case and test data. This model has a large gap in the strut in the vicinity of the midship section, as shown
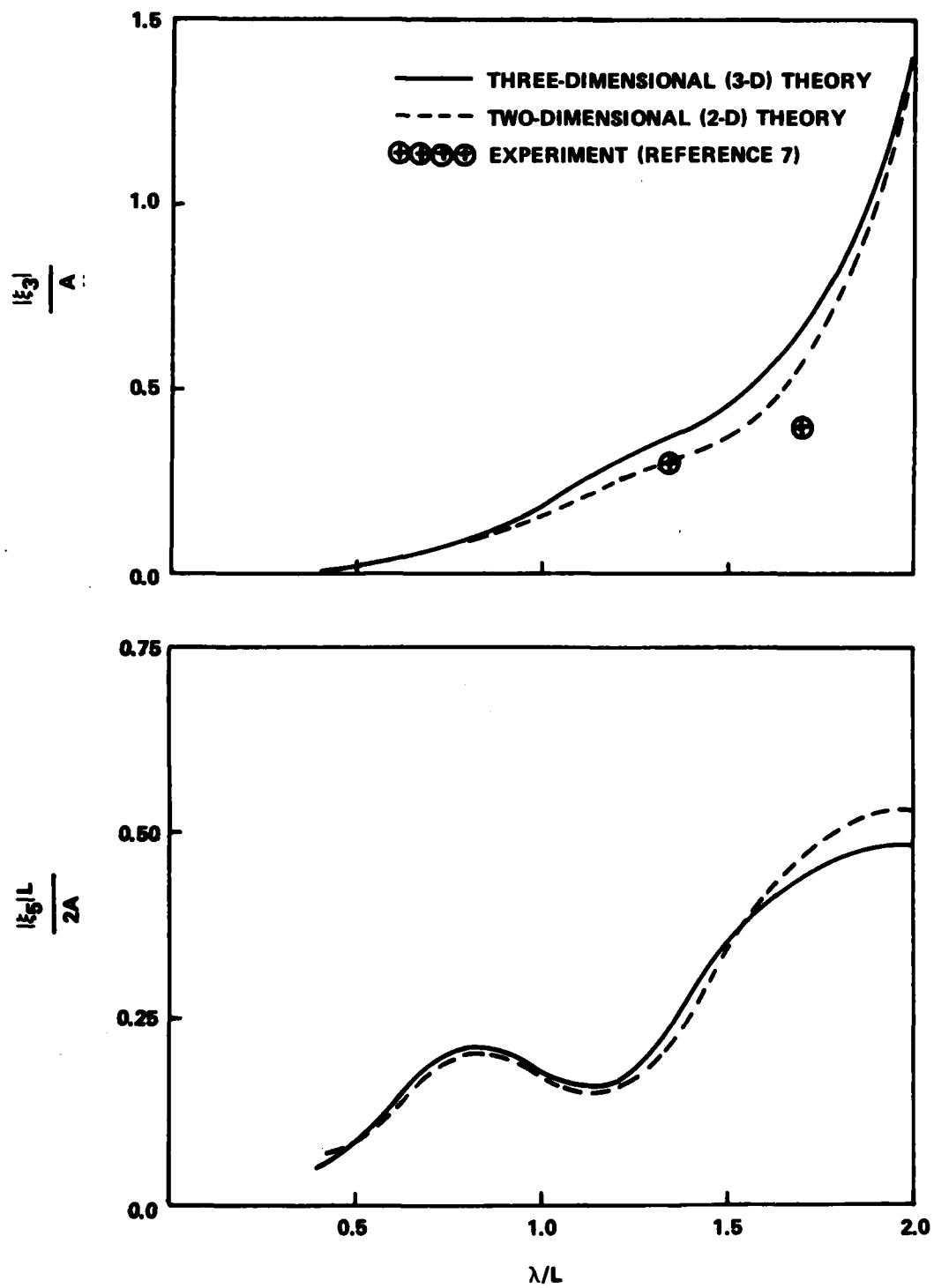
10

Figure 2 - Heave and Pitch Motions of SWATH 6A in Head Sea at
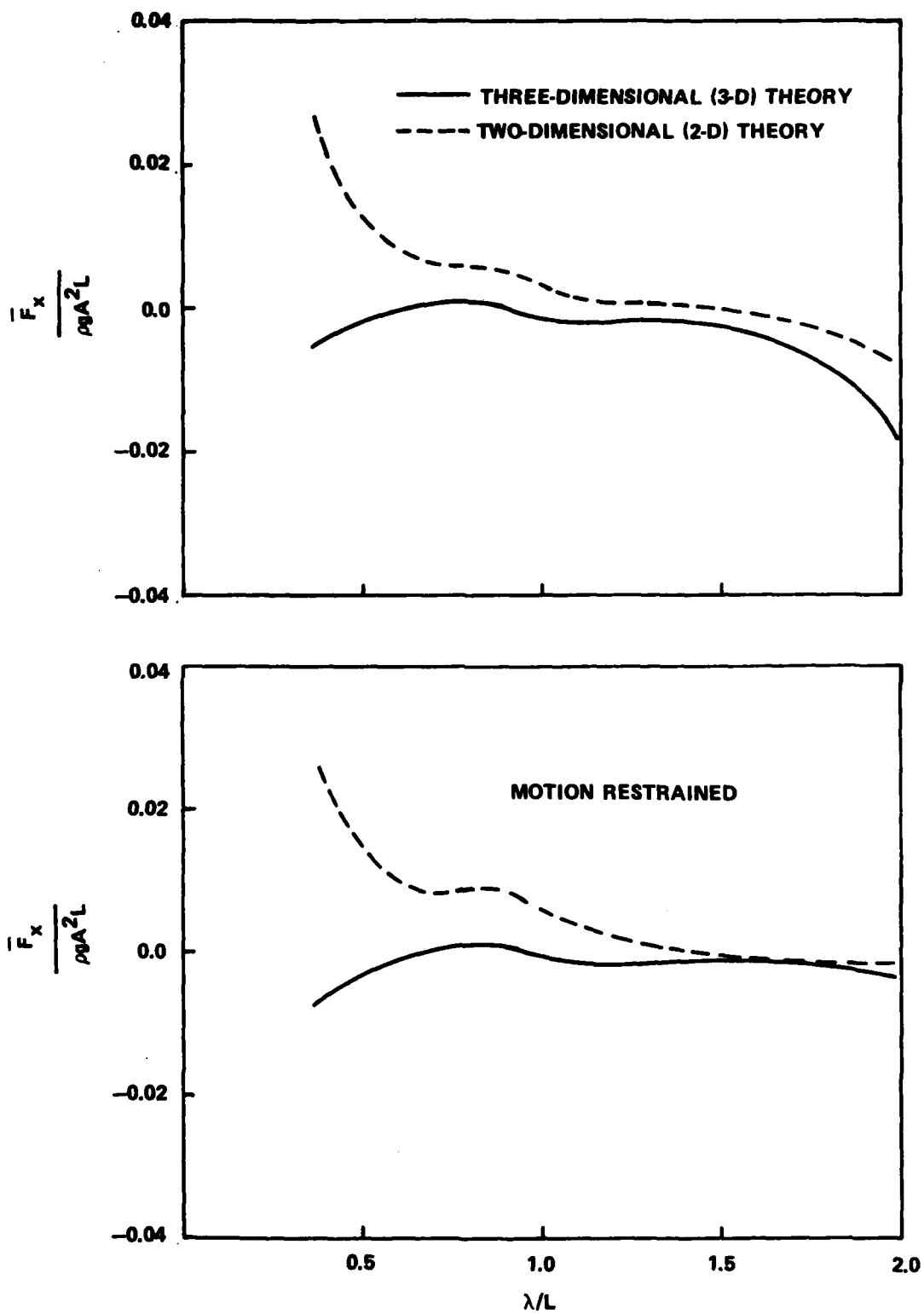Zero Forward Speed

11

Figure 3 – Surge Drift Force of SWATH 6A in Head Sea at
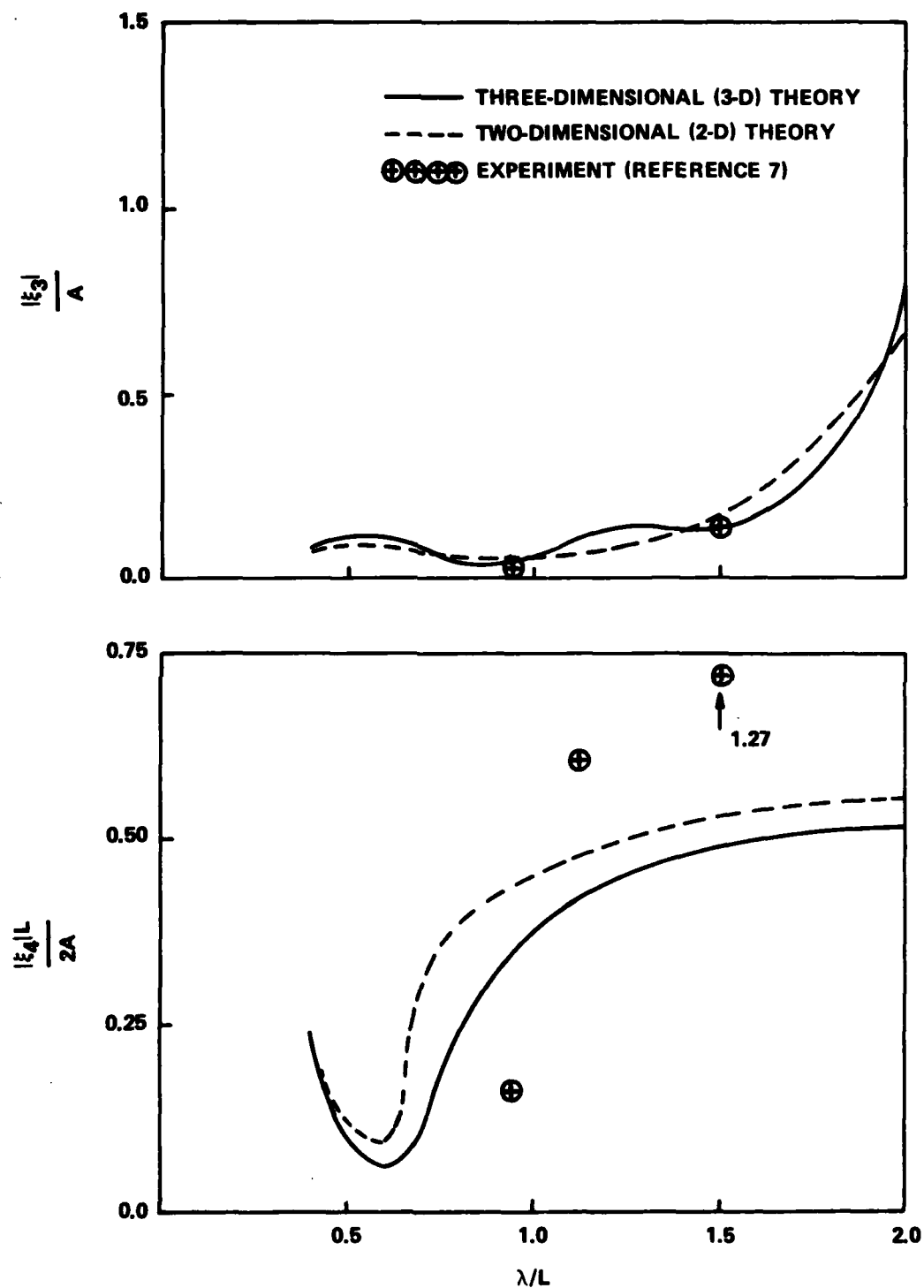Zero Forward Speed

12

Figure 4 – Heave and Roll Motions of SWATH 6A in Beam Sea at Zero Forward Speed
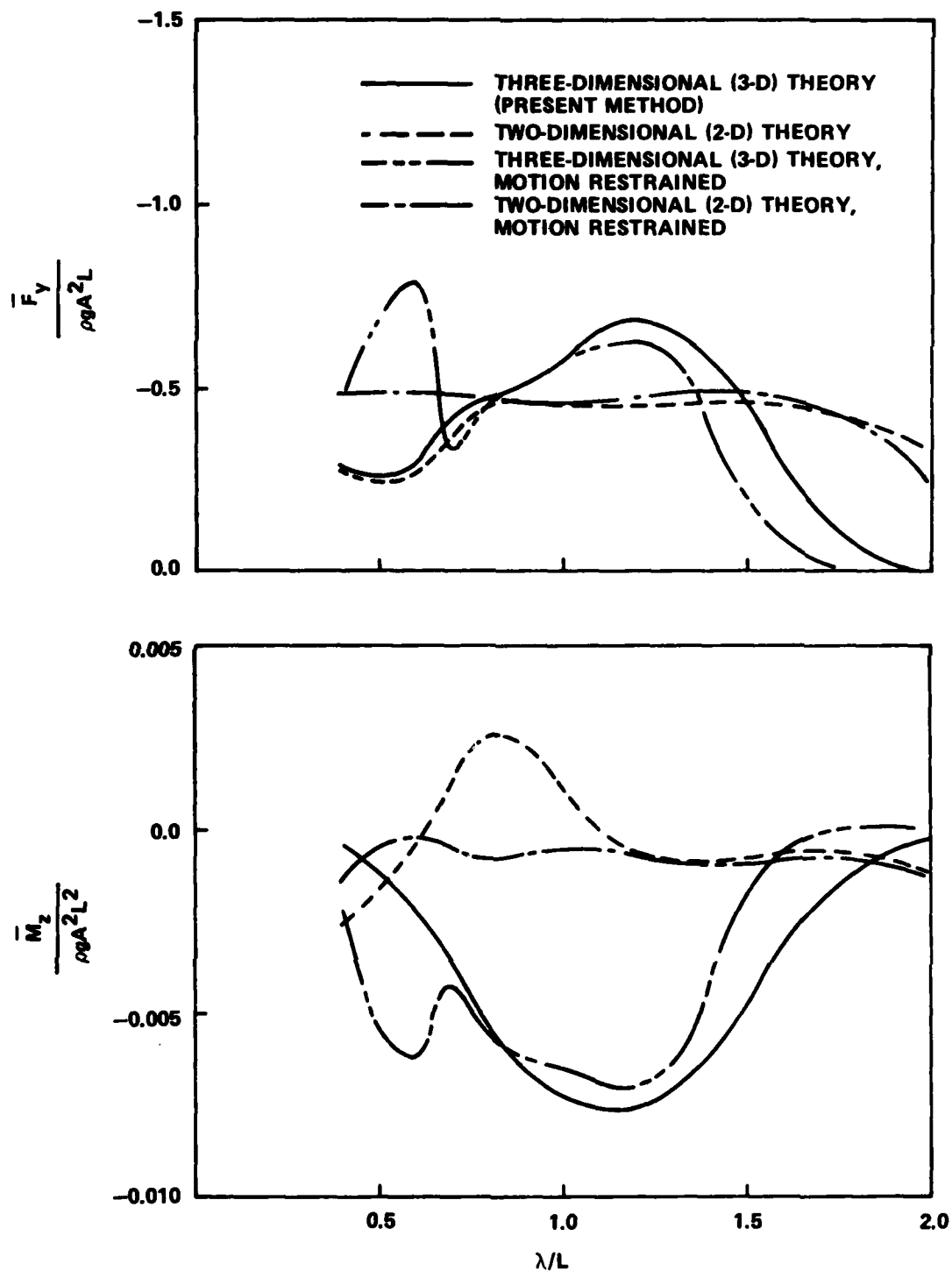
13

Figure 5 – Sway Drift Force and Yaw Drift Moment of SWATH 6A
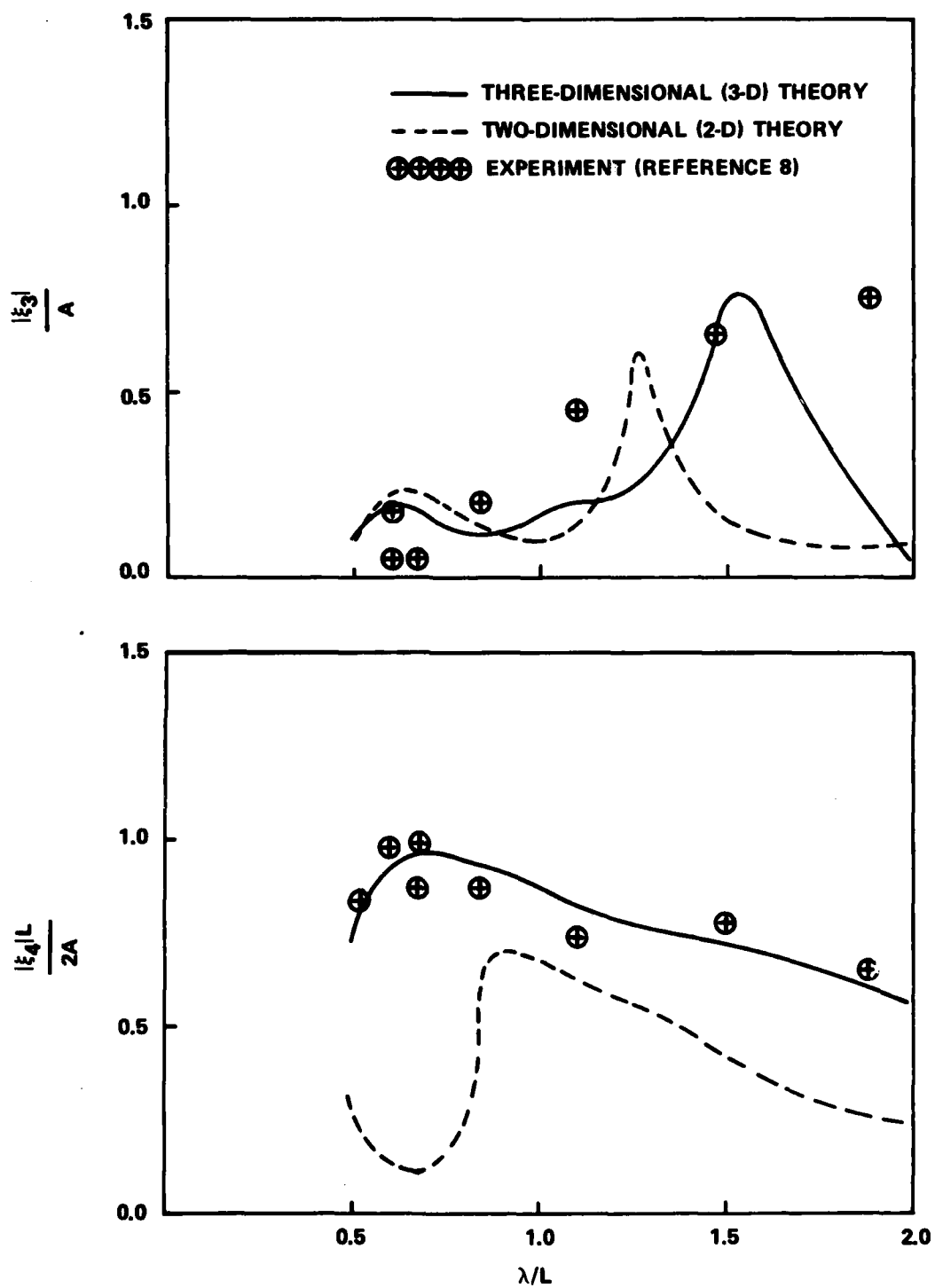in Beam Sea at Zero Forward Speed

14

Figure 6 – Heave and Roll Motions of Stretched SSP in Beam Sea at Zero Forward Speed
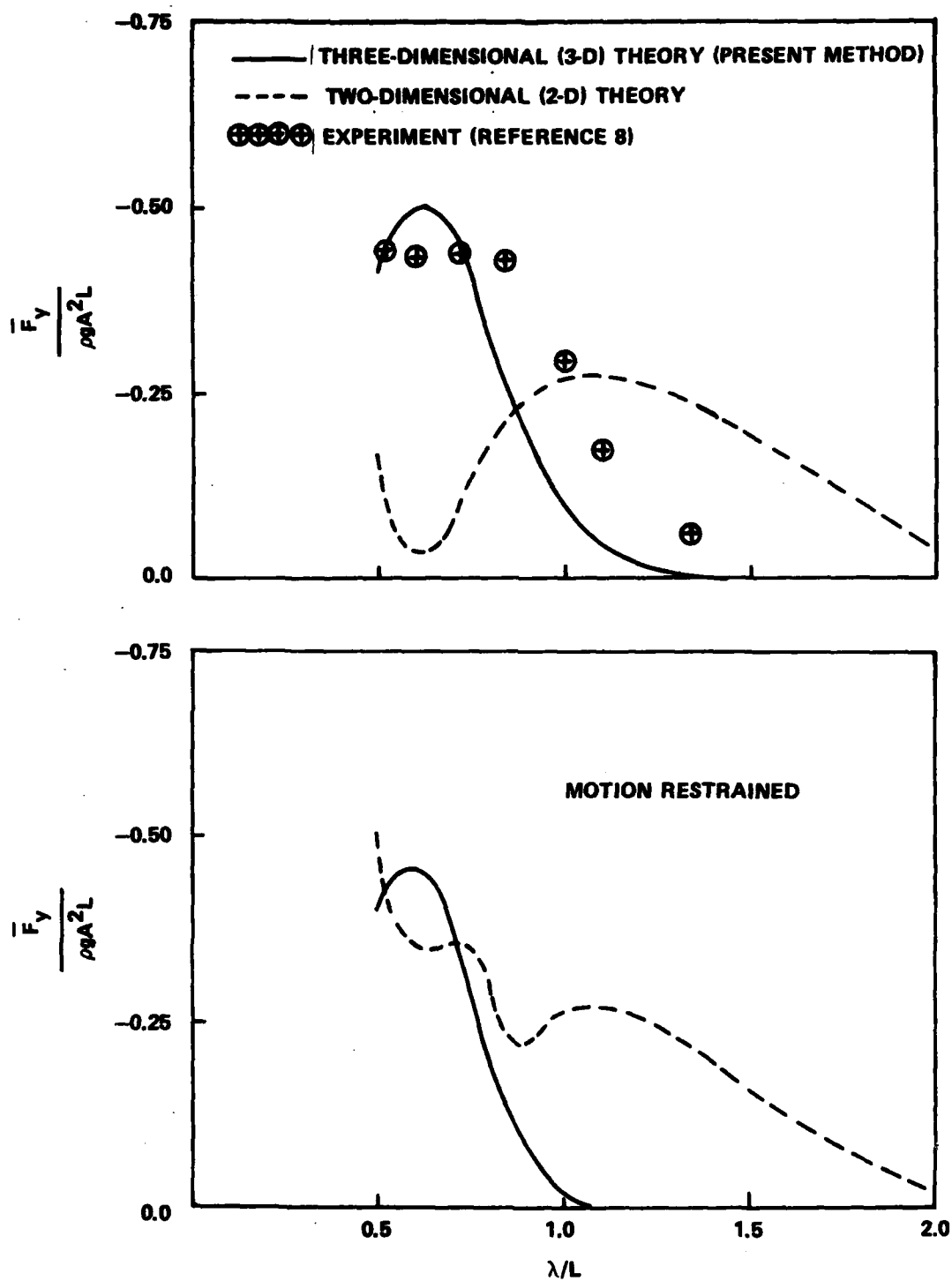
15

Figure 7 - Sway Drift Force of Stretched SSP in Bem Sea at
Zero Forward Speed

16

in Figure 8. In the two-dimensional modeling, the sections which have struts are modeled as floating; whereas those sections in the gap region are fully submerged. These interactions are not considered in the two-dimensional modeling. The three-dimensional approach takes these into account and models the interaction of sections fully. The discrepancies in roll motion between the two- and three-dimensional approaches are probably the result of these modeling differences and the interactions of these different sections. The results for SWATH 6A snd Stretched SSP indicate that the sectional interaction significantly affects the motion and drift force for the complicated shapes of these hull forms.

Figures 9 and 10 show the results of MCM 5371 in beam sea. Even though there are some minor differences in predicted roll motion between the two- and three-dimensional methods, the drift forces are nearly identical. Contrary to the SWATH ships, this hull has all floating sections. When the sections are of one type, in this case floating (surface intersecting), the interaction of the sections does not seem to affect the motion and drift force results. Compared with the experiment presented by O'Dea,[9] the computed results of drift force show good agreement when λ/L is larger than 0.3. As λ/L values become smaller, the discrepancy between the present method and experiment increases. The heave motion results show good agreement with the test results. However, the measured roll motion is too high and these are not plotted in Figure 9.

SUMMARY AND CONCLUSIONS

The three-dimensional method is applied to improve the computation of drift force and yaw moment for two SWATH ships and a surface ship. From the present study, the following conclusions may be drawn:

1. The numerical results of the three-dimensional method for the Stretched SSP show good agreement with experiment, whereas the result of applying the two-dimensional method is unsatisfactory for this model. Although the test results for SWATH 6A are not available for validation, it appears that for general SWATH ships the application of three-dimensional theory is more realistic, and the method shows better agreement with experimental data than the two-dimensional method.

2. For the surface ships, the results of two- and three-dimensional methods are almost identical and these results show good agreement with test data when λ/L is not too small.
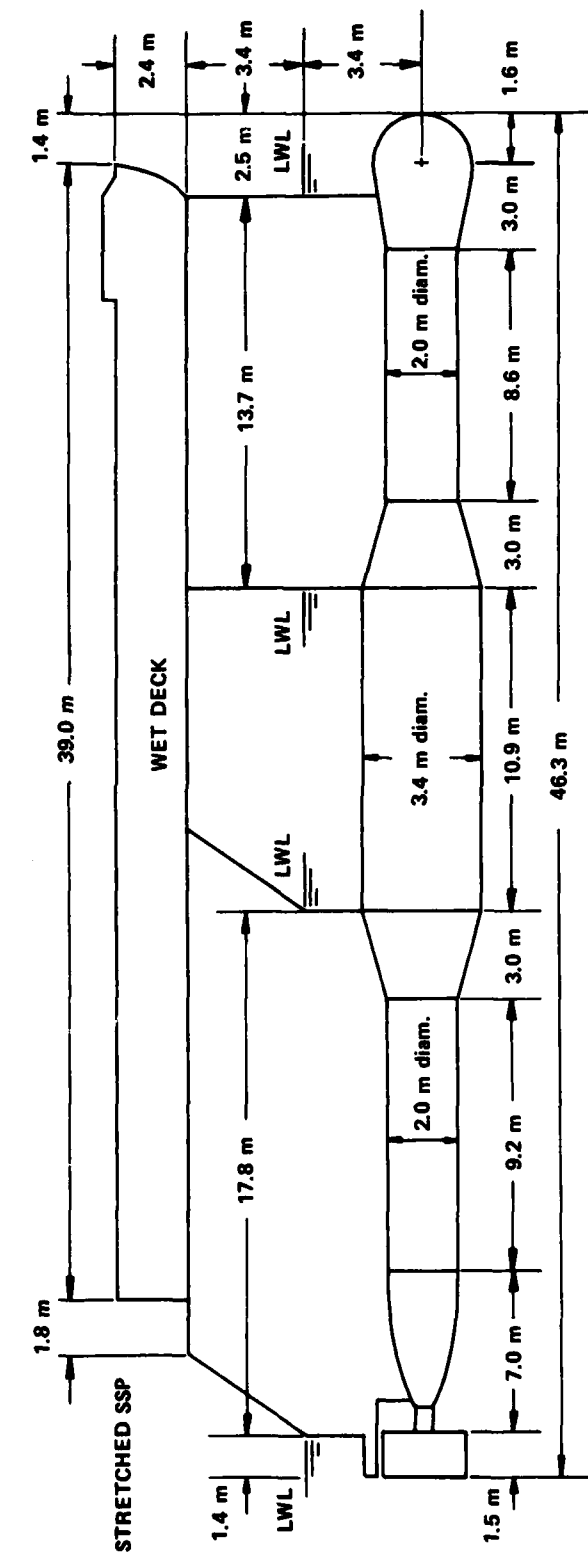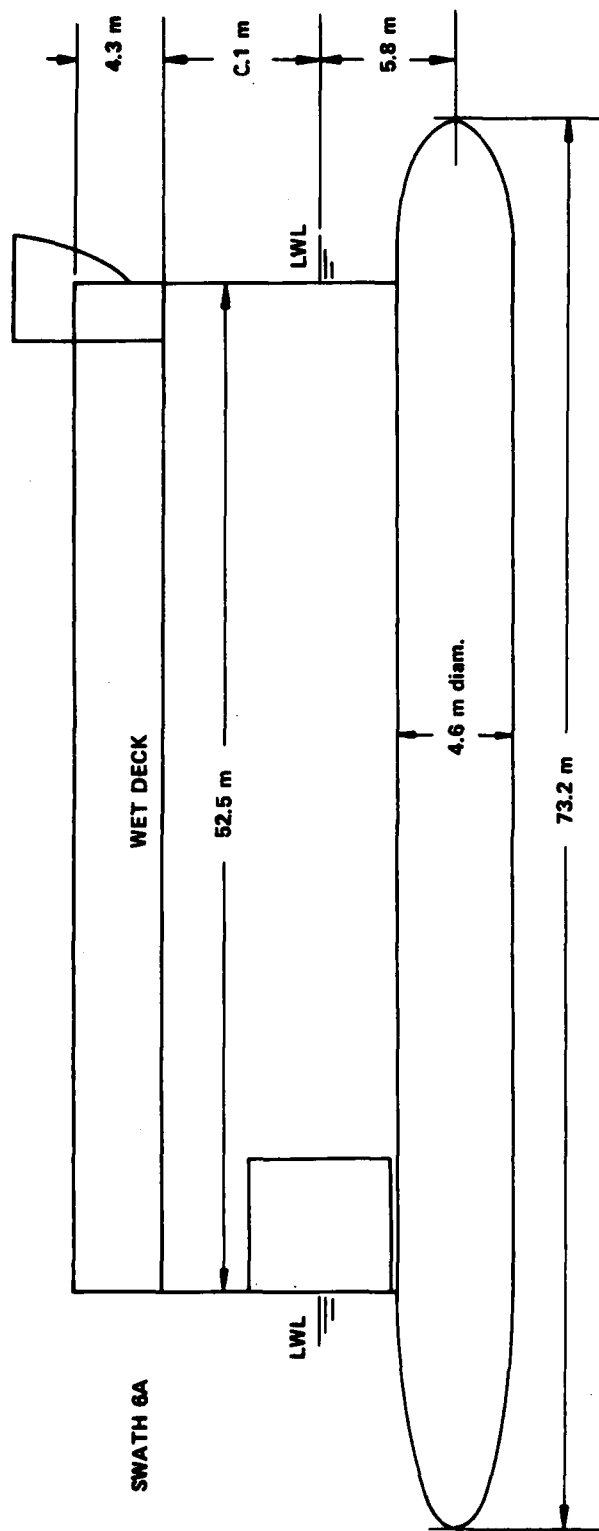
Figure 8 - Side Views of SWATH 6A and Stretched SSP
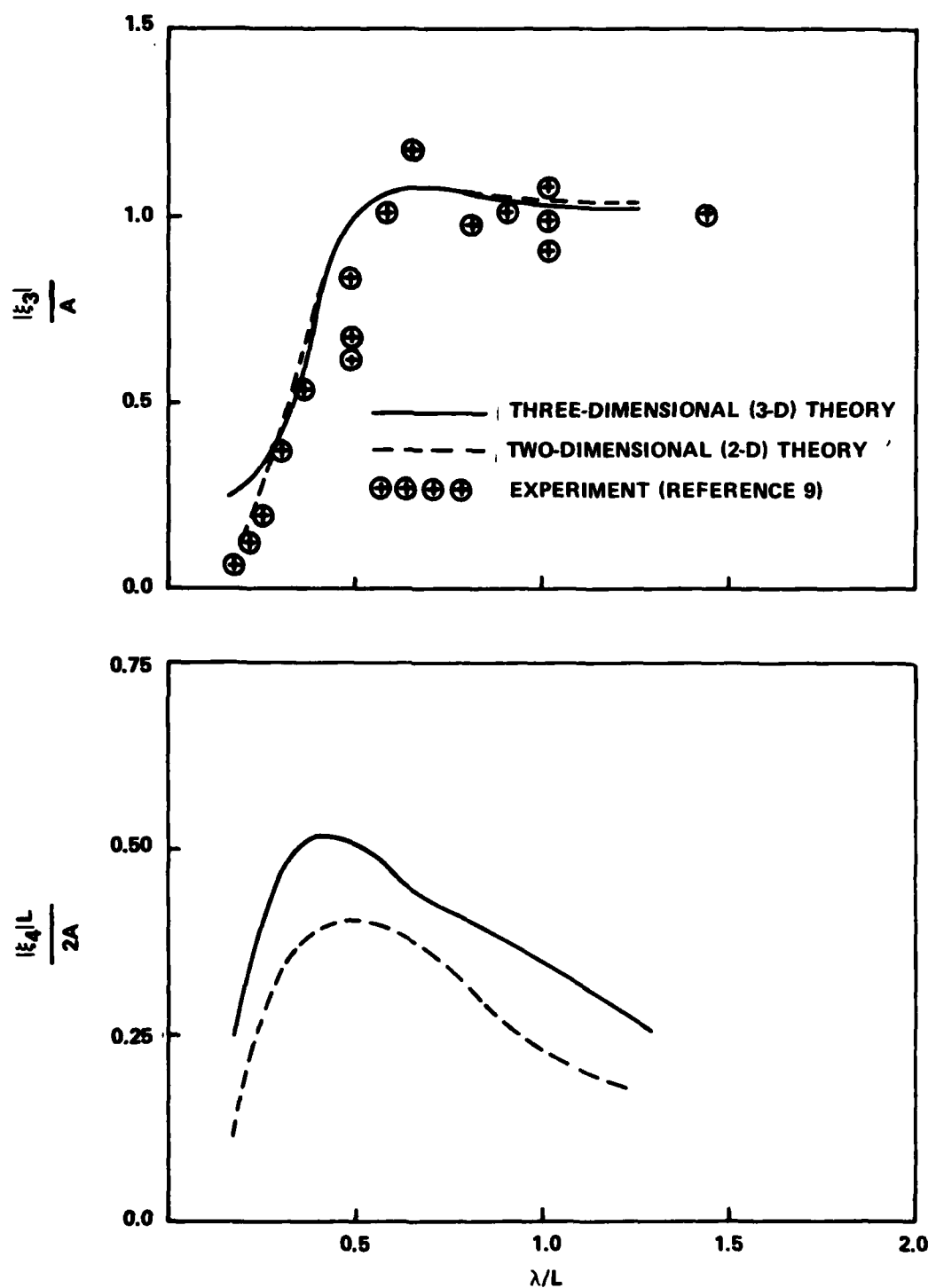
Figure 9 – Heave and Roll Motions of MCM 5371 in Beam Sea at
Zero Forward Speed
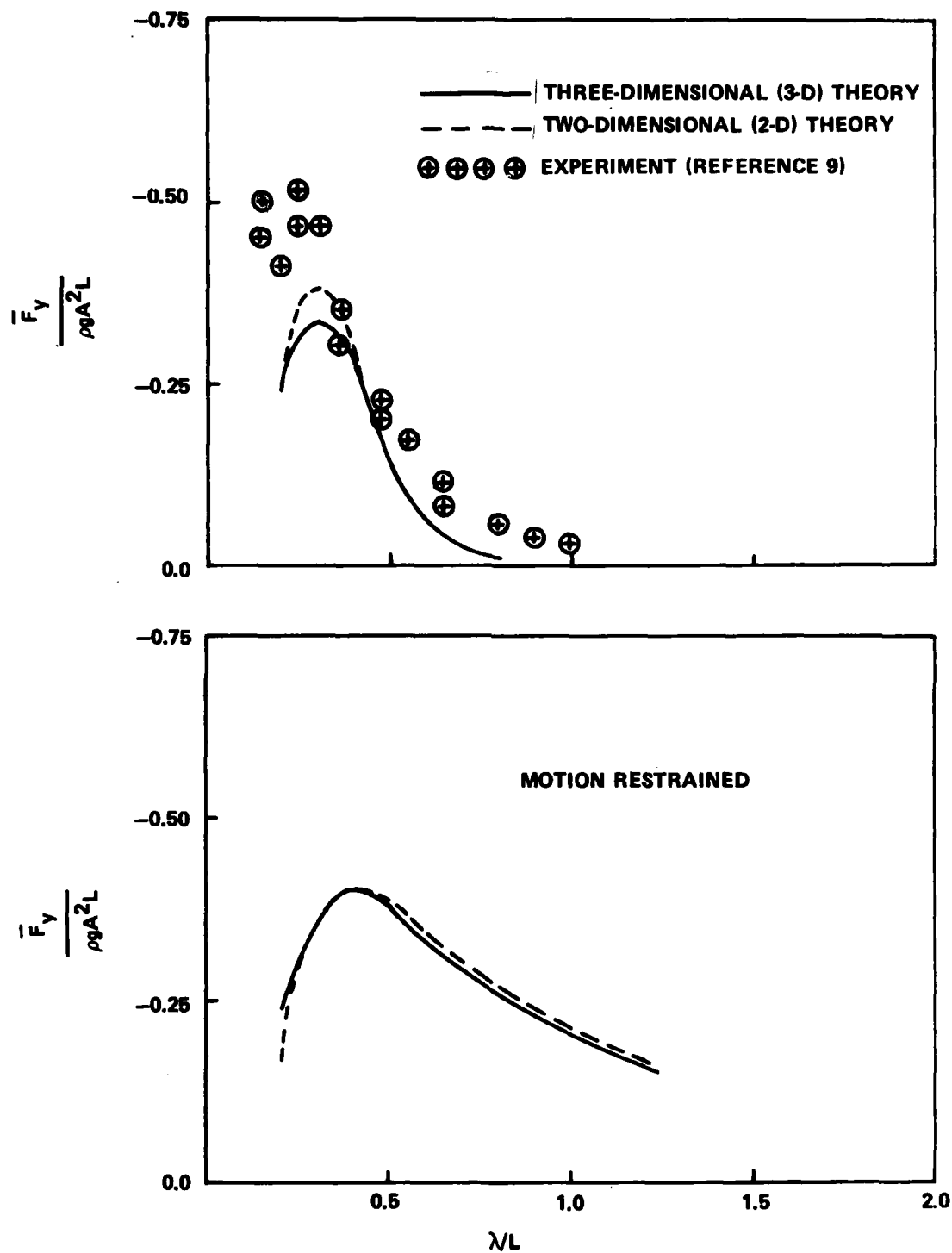
Figure 10 - Sway Drift Force of MCM 5371 in Beam Sea at Zero
Forward Speed

3. At the present time, the computational time for the three-dimensional program is fairly high. The computational time can be reduced in the future by reorganizing the present program and including creation of a master table of the Green functions.

4. The present study is restricted to the computation of drift force and moment for zero forward speed. The investigation of nonzero forward speed is highly recommended.

ACKNOWLEDGMENT

REFERENCES

1. Maruo, H., "The Drift of a Body Floating on Waves," Journal of Ship Research, Vol. 4, pp. 1-60 (Dec 1960).

2. Newman, J.N., "The Drift Force and Moment on Ships in Waves," Journal of Ship Research, Vol. 11, pp. 51-60 (Mar 1967).

3. Lee, C.M. and Y.H. Kim, "Prediction of Drift Force on Twin Hull Bodies in Waves," Report DTNSRDC-82/018 (Feb 1982).

4. Hong, Y.S. and J.R. Paulling, "A Procedure for the Computation of Wave- and Motion-Induced Forces on Three-Dimensional Bodies at Zero Forward Motion," Prepared for American Bureau of Shipping (May 1979).

5. Wehausen, J.V. and E.V. Laitone, "Surface Waves," in Handbuch der Phys., Vol. 9, pp. 446-778 (1960).

6. Stoker, J.J., "Water Waves," Interscience Pub. Inc., New York (1957).

7. Kallio, J.A., "Seaworthiness Characteristics of A 2900 Ton Small Waterplane Area Twin Hull (SWATH)," Report DTNSRDC/SPD-620-03 (Sep 1976).

8. Numata, E., "Model Test of Stretched SSP," Stevens Institute of Technology, Davidson Lab. Report SIT-DL-81-9-2158 (May 1981).

9. O'Dea, J., DTNSRDC Report in preparation.

APPENDIX A

DERIVATION OF EQUATIONS FOR DRIFT FORCES AND MOMENT

The derivation of Equations (28)-(30) is given in Reference 1. Since the potential of the incoming wave is expressed differently in this presentation from that given in Reference 1, more details of derivation are presented in this appendix. In the following, an asterisk denotes the complex conjugate, the prime denotes a derivative with respect to θ, and Re and Im denote the real and imaginary parts of a complex function, respectively.

In the polar coordinate system, the velocity components are

$$V_x = V_R \cos \theta - V_\theta \sin \theta \tag{A.1}$$

$$V_y = V_R \sin \theta + V_\theta \cos \theta \tag{A.2}$$

$$V_n = - V_R \tag{A.3}$$

Substituting these equations into Equations (24), (25), and (26), we obtain

$$\bar{F}_x = - \iint_{S_\infty} \overline{[p \cos \theta + \rho V_R (V_R \cos \theta - V_\theta \sin \theta)]} \, R \, d\theta \, dz \tag{A.4}$$

$$\bar{F}_y = - \iint_{S_\infty} \overline{[p \sin \theta + \rho V_R (V_R \sin \theta + V_\theta \cos \theta)]} \, R \, d\theta \, dz \tag{A.5}$$

$$\bar{M}_z = - \iint_{S_\infty} \overline{\rho \, V_R \, V_\theta \, R^2} \, d\theta \, dz \tag{A.6}$$

where the superscript bar denotes time averaging over the wave period. The radial and tangential velocity components are

$$V_R = \text{Re} \left(\frac{\partial \phi}{\partial R} e^{-i\omega t} \right) \tag{A.7}$$

25

$$V_\theta = \text{Re} \left(\frac{1}{R} \frac{\partial \phi}{\partial \theta} e^{-i\omega t} \right) \qquad (A.8)$$

The far-field potentials are

$$\phi_I = - \frac{igA}{\omega} \exp[Kz + iKR \cos(\beta+\theta)] \qquad (A.9)$$

$$\phi_B = \left(\frac{K}{2\pi R} \right)^{1/2} H(\pi+\theta) \exp\left(Kz + iKR + i\frac{\pi}{4} \right) \qquad (A.10)$$

Equation (A.9) is the expression of Equation (2) in polar coordinates and ϕ_B is given in Reference 1. Since, in the far-field, both ϕ_I and ϕ_B are exponential functions in z, it is convenient to integrate Equations (A.4)-(A.6) with respect to z. The upper limit of this integration is the free surface height

$$z = \zeta = - \frac{1}{g} \left. \Phi_t \right|_{z=0} = \text{Re}\left[\frac{i\omega}{g} \phi(x,y,o) e^{-i\omega t} \right] \qquad (A.11)$$

and it follows that

$$\overline{\int_{-\infty}^{\zeta} p \, dz} = \overline{\rho \, \zeta \, \text{Re}[i\omega\phi(x,y,o)e^{-i\omega t}]} - \overline{\frac{\rho}{4K} |\vec{v}|^2} - \overline{\frac{1}{2} \rho g \zeta^2} \qquad (A.12)$$

The first and the third terms of Equation (A.12) become

$$\overline{\left\{ \rho\zeta \, \text{Re}[i\omega\phi(x,y,o)e^{-i\omega t}] - \frac{\rho g}{2} \zeta^2 \right\}}$$

$$= \overline{\left\{ \frac{\rho}{g} [\text{Re}(i\omega\phi e^{-i\omega t})]^2 - \frac{\rho g}{2} \left[\text{Re}\left(\frac{i\omega}{g} \phi \, e^{-i\omega t} \right) \right]^2 \right\}} \qquad (A.13)$$

$$= \overline{\frac{\rho}{2g} [\text{Re}(i\omega\phi e^{-i\omega t})]^2} = \frac{\rho K}{4} |\phi|^2_{z=o}$$

26

The second term becomes

$$-\overline{\frac{\rho}{4K}\,|\vec{v}|^2} = -\frac{\rho}{8K}\left(\left|\frac{\partial\phi}{\partial R}\right|^2 + \frac{1}{R^2}\left|\frac{\partial\phi}{\partial\theta}\right|^2 + K^2|\phi|^2\right)_{z=0} \qquad (A.14)$$

The integration of V_R and $V_R V_\theta$ in Equations (A.4)-(A.6) are given by

$$\overline{\int_{-\infty}^{\zeta} V_R^2\,dz} = \overline{\frac{1}{2K}\,(V_R^2)}_{z=0} = \frac{1}{4K}\left|\frac{\partial\phi}{\partial R}\right|^2_{z=0} \qquad (A.15)$$

$$\overline{\int_{-\infty}^{\zeta} V_R V_\theta\,dz} = \overline{\frac{1}{2K}\,(V_R V_\theta)}_{z=0} = \frac{1}{8KR}\left(\frac{\partial\phi}{\partial R}\frac{\partial\phi^*}{\partial\theta} + \frac{\partial\phi^*}{\partial R}\frac{\partial\phi}{\partial\theta}\right)_{z=0} \qquad (A.16)$$

Substituting Equations (A.13)-(A.16) into Equations (A.4)-(A.6), we obtain the forces and moment in terms of the velocity potential

$$\bar{F}_x = \frac{\rho}{8K}\int_0^{2\pi}\left(\frac{1}{R^2}\frac{\partial\phi}{\partial\theta}\frac{\partial\phi^*}{\partial\theta} - \frac{\partial\phi}{\partial R}\frac{\partial\phi^*}{\partial R} - K^2\phi\phi^*\right) R\cos\theta\,d\theta$$

$$+ \frac{\rho}{8K}\int_0^{2\pi}\left(\frac{\partial\phi}{\partial R}\frac{\partial\phi^*}{\partial\theta} + \frac{\partial\phi^*}{\partial R}\frac{\partial\phi}{\partial\theta}\right)\sin\theta\,d\theta \qquad (A.17)$$

$$\bar{F}_y = \frac{\rho}{8K}\int_0^{2\pi}\left(\frac{1}{R^2}\frac{\partial\phi^*}{\partial\phi}\frac{\partial\phi}{\partial\theta} - \frac{\partial\phi}{\partial R}\frac{\partial\phi^*}{\partial R} - K^2\phi\phi^*\right) R\sin\theta\,d\theta$$

$$- \frac{\rho}{8K}\int_0^{2\pi}\left(\frac{\partial\phi}{\partial R}\frac{\partial\phi^*}{\partial\theta} + \frac{\partial\phi^*}{\partial R}\frac{\partial\phi}{\partial\theta}\right)\cos\theta\,d\theta \qquad (A.18)$$

27

$$\bar{M}_z = - \frac{\rho}{8K} \int_0^{2\pi} \left(\frac{\partial \phi}{\partial R} \frac{\partial \phi^*}{\partial \theta} + \frac{\partial \phi^*}{\partial R} \frac{\partial \phi}{\partial \theta} \right) R \, d\theta \tag{A.19}$$

In the above equations, the potential, its derivatives, and their conjugates are computed at $z = 0$. Employing the definition $\phi = \phi_I + \phi_B$, Equations (A.9) and (A.10) are substituted into the force and moment equations. The first term of Equation (A.17) becomes zero as $R \to \infty$. The remainder of the terms can be expressed in integral form as

$$\int_0^{2\pi} \frac{\partial \phi}{\partial R} \frac{\partial \phi^*}{\partial R} R \cos \theta \, d\theta = \int_0^{2\pi} \left(\frac{\partial \phi_I}{\partial R} \frac{\partial \phi^*_I}{\partial R} + \frac{\partial \phi_B}{\partial R} \frac{\partial \phi^*_B}{\partial R} + \frac{\partial \phi_I}{\partial R} \frac{\partial \phi^*_B}{\partial R} + \frac{\partial \phi^*_I}{\partial R} \frac{\partial \phi_B}{\partial R} \right) R \cos \theta \, d\theta$$

$$= \frac{K^3}{2\pi} \int_0^{2\pi} H(\pi+\theta) \, H^*(\pi+\theta) \cos \theta \, d\theta - 2\omega \, AK \left(\frac{KR}{2\pi} \right)^{1/2} \mathrm{Im} \int_0^{2\pi} \cos(\beta+\theta) \cos \theta \, H(\pi+\theta) d\theta$$

$$\times \exp \left[-i \, KR \cos(\beta+\theta) + i \, KR + i \, \frac{\pi}{4} \right] \tag{A.20}$$

$$\int_0^{2\pi} K^2 \, \phi \, \phi^* R \cos \theta \, d\theta = K^2 \int_0^{2\pi} (\phi_I \phi_I^* + \phi_B \phi_B^* + \phi_I \phi_B^* + \phi_I^* \phi_B) \, R \cos \theta \, d\theta$$

$$= \frac{K^3}{2\pi} \int_0^{2\pi} H(\pi+\theta) \, H^*(\pi+\theta) \cos \theta \, d\theta - 2\omega \, AK \left(\frac{KR}{2\pi} \right)^{1/2} \mathrm{Im} \int_0^{2\pi} H(\pi+\theta) \cos \theta \, d\theta$$

$$\times \exp \left[-i \, KR \cos(\beta+\theta) + i \, KR + i \, \frac{\pi}{4} \right] \tag{A.21}$$

$$\int_0^{2\pi} \frac{\partial\phi}{\partial R} \frac{\partial\phi^*}{\partial\theta} \sin\theta \, d\theta = \int_0^{2\pi} \left(\frac{\partial\phi_I}{\partial R} \frac{\partial\phi^*_I}{\partial\theta} + \frac{\partial\phi_I}{\partial R} \frac{\partial\phi^*_B}{\partial\theta} + \frac{\partial\phi_B}{\partial R} \frac{\partial\phi^*_I}{\partial\theta} + \frac{\partial\phi_B}{\partial R} \frac{\partial\phi^*_B}{\partial\theta} \right) \sin\theta \, d\theta$$

$$= - i \, \omega \, AK \left(\frac{KR}{2\pi} \right)^{1/2} \int_0^{2\pi} H(\pi+\theta) \, \sin(\beta+\theta) \, \sin\theta \, \exp\left[-iKR \cos(\beta+\theta)+iKR+i\,\frac{\pi}{4} \right] d\theta$$

$$\text{(A.22)}$$

$$\int_0^{2\pi} \frac{\partial\phi^*}{\partial R} \frac{\partial\phi}{\partial\theta} \sin\theta \, d\theta = \int_0^{2\pi} \left(\frac{\partial\phi^*_I}{\partial R} \frac{\partial\phi_I}{\partial\theta} + \frac{\partial\phi^*_I}{\partial R} \frac{\partial\phi_B}{\partial\theta} + \frac{\partial\phi^*_B}{\partial R} \frac{\partial\phi_I}{\partial\theta} + \frac{\partial\phi^*_B}{\partial R} \frac{\partial\phi_B}{\partial\theta} \right) \sin\theta \, d\theta$$

$$= i \, \omega \, AK \left(\frac{KR}{2\pi} \right)^{1/2} \int_0^{2\pi} H^*(\pi+\theta) \, \sin(\beta+\theta) \, \sin\theta \, \exp\left[iKR \cos(\beta+\theta)-iKR-i\,\frac{\pi}{4} \right] d\theta$$

$$\text{(A.23)}$$

With substitution of Equations (A.20)-(A.23) into Equations (A.17) and (A.18), the forces are

$$\bar{F}_x = - \frac{\rho K^2}{8\pi} \int_0^{2\pi} |H(\pi+\theta)|^2 \cos\theta \, d\theta + \frac{\rho\omega A}{4} \left(\frac{KR}{2\pi} \right)^{1/2} \text{Im} \int_0^{2\pi} H(\pi+\theta) \, (\cos\theta+\cos\beta) \, d\theta$$

$$\times \exp\left[-iKR \cos(\beta+\theta)+iKR+i\,\frac{\pi}{4} \right] \qquad\qquad \text{(A.24)}$$

$$\bar{F}_y = - \frac{\rho K^2}{8\pi} \int_0^{2\pi} |H(\pi+\theta)|^2 \sin\theta \, d\theta + \frac{\rho\omega A}{4} \left(\frac{KR}{2\pi} \right)^{1/2} \text{Im} \int_0^{2\pi} H(\pi+\theta) \, (\sin\theta-\sin\beta) \, d\theta$$

$$\times \exp\left[-iKR \cos(\beta+\theta)+iKR+i\,\frac{\pi}{4} \right] \qquad\qquad \text{(A.25)}$$

The integral terms of Equation (A.19) can be written as

$$\int_0^{2\pi} \frac{\partial \phi}{\partial R} \frac{\partial \phi^*}{\partial \theta} R \, d\theta = \int_0^{2\pi} \left(\frac{\partial \phi_I}{\partial R} \frac{\partial \phi^*_I}{\partial \theta} + \frac{\partial \phi_I}{\partial R} \frac{\partial \phi^*_B}{\partial \theta} + \frac{\partial \phi_B}{\partial R} \frac{\partial \phi^*_I}{\partial \theta} + \frac{\partial \phi_B}{\partial R} \frac{\partial \phi^*_B}{\partial \theta} \right) R \, d\theta$$

$$= \omega A \left(\frac{KR}{2\pi} \right)^{1/2} \int_0^{2\pi} H^{*\prime}(\pi+\theta) \cos(\beta+\theta) \exp\left[iKR \cos(\beta+\theta) - iKR - i\frac{\pi}{4} \right] d\theta$$

$$- \omega A \left(\frac{KR}{2\pi} \right)^{1/2} \left(-\frac{1}{2} + iKR \right) \int_0^{2\pi} H(\pi+\theta) \sin(\beta+\theta) \exp\left[-iKR \cos(\beta+\theta) + iKR + i\frac{\pi}{4} \right] d\theta$$

$$+ \frac{i \, K^2}{2\pi} \int_0^{2\pi} H(\pi+\theta) \, H^{*\prime}(\pi+\theta) \, d\theta \qquad\qquad (A.26)$$

$$\int_0^{2\pi} \frac{\partial \phi^*}{\partial R} \frac{\partial \phi}{\partial \theta} R \, d\theta = \int_0^{2\pi} \left(\frac{\partial \phi^*_I}{\partial R} \frac{\partial \phi_I}{\partial \theta} + \frac{\partial \phi^*_I}{\partial R} \frac{\partial \phi_B}{\partial \theta} + \frac{\partial \phi^*_B}{\partial R} \frac{\partial \phi_I}{\partial \theta} + \frac{\partial \phi^*_B}{\partial R} \frac{\partial \phi_B}{\partial \theta} \right) R \, d\theta$$

$$= \omega A \left(\frac{KR}{2\pi} \right)^{1/2} \int_0^{2\pi} H^{\prime}(\pi+\theta) \cos(\beta+\theta) \exp\left[-iKR \cos(\beta+\theta) + iKR + i\frac{\pi}{4} \right] d\theta$$

$$+ \omega A \left(\frac{KR}{2\pi} \right)^{1/2} \left(\frac{1}{2} + iKR \right) \int_0^{2\pi} H^{*}(\pi+\theta) \sin(\beta+\theta) \exp\left[iKR \cos(\beta+\theta) - iKR - i\frac{\pi}{4} \right] d\theta$$

$$- i \, \frac{K^2}{2\pi} \int_0^{2\pi} H^{*}(\pi+\theta) \, H^{\prime}(\pi+\theta) \, d\theta \qquad\qquad (A.27)$$

30

Substitution of these two equations into Equation (A.19) yields the moment as

$$\bar{M}_z = -\frac{\rho K}{8\pi} \, \text{Im} \int_0^{2\pi} H^*(\pi+\theta) \, H'(\pi+\theta) \, d\theta - \frac{\rho g A}{4\omega} \left(\frac{KR}{2\pi}\right)^{1/2} \text{Re} \int_0^{2\pi} H'(\pi+\theta) \, d\theta$$

$$\times \, [1+\cos(\beta+\theta)] \, \exp\left[-iKR \, \cos(\beta+\theta)+iKR+i\,\frac{\pi}{4}\right] \tag{A.28}$$

The integrals in Equations (A.24), (A.25), and (A.28) involving R can be evaluated by the method of stationary phase. When R is large, the following integral is integrated as (see Reference 6)

$$\int_a^b \psi(\xi,R) e^{iR\varphi(\xi)} \, d\xi = \Sigma \, \psi(\alpha_r,R) \left[\frac{2\pi}{R|\varphi''(\alpha_r)|}\right]^{1/2} \exp\left[iR\varphi(\alpha_r)\pm i\,\frac{\pi}{4}\right]$$

$$+ \sum_S \psi(\alpha_s,R) \, \frac{\Gamma(1/3)}{\sqrt{3}} \left[\frac{6}{R|\varphi'''(\alpha_s)|}\right]^{1/3} \exp[iR\varphi(\alpha_s)]$$

$$\varphi'(\alpha_r) = 0, \; \varphi''(\alpha_r) \neq 0 \begin{cases} + \text{ sign when } \varphi''(\alpha_r) > 0 \\ \\ - \text{ sign when } \varphi''(\alpha_r) < 0 \end{cases}$$

$$\varphi'(\alpha_s) = 0, \; \varphi''(\alpha_s) = 0, \; \varphi'''(\alpha_s) \neq 0 \tag{A.29}$$

Therefore, the exponential integral becomes

$$\int_0^{2\pi} f(\theta) \, \exp[-iKR \, \cos(\beta+\theta)] \, d\theta$$

$$= \left(\frac{2\pi}{KR}\right)^{1/2} [f(-\beta) e^{-iKR+i(\pi/4)}+f(\pi-\beta) e^{-KR-i(\pi/4)}] \tag{A.30}$$

31

and the integrals in the equations of the forces and moment are evaluated as follows

$$\int_0^{2\pi} H(\pi+\theta) \, (\cos\theta+\cos\beta) \, \exp\left[-iKR\cos(\beta+\theta)+iKR+i\frac{\pi}{4}\right] d\theta$$

$$= \left(\frac{2\pi}{KR}\right)^{1/2} 2i \, \cos\beta \, H(\pi-\beta) \qquad (A.31)$$

$$\int_0^{2\pi} H(\pi+\theta) \, (\sin\theta-\sin\beta) \, \exp\left[-iKR\cos(\beta+\theta)+iKR+i\frac{\pi}{4}\right] d\theta$$

$$= -\left(\frac{2\pi}{KR}\right)^{1/2} 2i \, \sin\beta \, H(\pi-\beta) \qquad (A.32)$$

$$\int_0^{2\pi} H'(\pi+\theta) \, [1+\cos(\beta+\theta)] \, \exp\left[-iKR\cos(\beta+\theta)+iKR+i\frac{\pi}{4}\right] d\theta$$

$$= \left(\frac{2\pi}{KR}\right)^{1/2} 2i \, H'(\pi-\beta) \qquad (A.33)$$

With the substitution of Equations (A.31)-(A.33) into Equations (A.24), (A.25), and (A.28), respectively, the equations of forces and moment are given in final form as

$$\bar{F}_x = -\frac{\rho K^2}{8\pi} \int_0^{2\pi} |H(\pi+\theta)|^2 \cos\theta \, d\theta + \frac{\rho\omega A}{2} \cos\beta \, Re[H(\pi-\beta)] \qquad (A.34)$$

$$\bar{F}_y = -\frac{\rho K^2}{8\pi} \int_0^{2\pi} |H(\pi+\theta)|^2 \sin\theta \, d\theta - \frac{\rho\omega A}{2} \sin\beta \, Re[H(\pi-\beta)] \qquad (A.35)$$

$$\bar{M}_z = -\frac{\rho K}{8\pi} \, Im \int_0^{2\pi} H^*(\pi+\theta) \, H'(\pi+\theta) \, d\theta + \frac{\rho\omega A}{2K} \, Im[H'(\pi-\beta)] \qquad (A.36)$$

32

APPENDIX B

DERIVATION OF EXCITING FORCES IN TERMS OF KOCHIN FUNCTION

The exciting forces are computed by integrating the pressure due to incoming wave diffraction potentials over the wetted surface as

$$F_j = - \iint_{S_B} p \, n_j \, dS = \iint_{S_B} (-i\rho\omega) \, (\varphi_7 + \phi_I) \, n_j \, dS \qquad (B.1)$$

From the body boundary condition (Equation (5)), F_j becomes

$$F_j = \rho \iint_{S_B} \varphi_{jn} \, (\varphi_7 + \phi_I) \, dS \qquad (B.2)$$

Applying Green's identity, we obtain

$$F_j = \rho \iint_{S_B} \left(\varphi_{jn}\phi_I + \varphi_j \frac{\partial \varphi_7}{\partial n} \right) dS \qquad (B.3)$$

From the body boundary condition for the diffraction potential (Equation (6)), F_j is given by

$$F_j = \rho \iint_{S_B} \left(\varphi_{jn} - \varphi_j \frac{\partial}{\partial n} \right) \phi_I \, dS \qquad (B.4)$$

We substitute Equation (2) for ϕ_I, and finally have the exciting forces as

$$F_j = - \frac{i\rho gA}{\omega} \iint_{S_B} \left(\varphi_{jn} - \varphi_j \frac{\partial}{\partial n} \right) e^{Kz} \exp(iKx \cos \beta - iKy \sin \beta) \, dS$$

$$= \frac{i\rho gA}{\omega} H_j(-\beta) \qquad (B.5)$$

33

INITIAL DISTRIBUTION

Copies		Copies	

Copies

1   CHONR/432/C.M. Lee

2   NRL
   1   Code 2027
   1   Code 2627

3   USNA
   1   Tech Lib
   1   Nav Sys Eng Dept
   1   Bhattacheryya

2   NAVPGSCOL
   1   Library
   1   Garrison

1   NADC

1   NELC/Lib

1   NOSC
   1   Library

1   NCEL/Code 131
   Port Hueneme, CA   93043

13   NAVSEA
   1   SEA 501/G. Kerr
   1   SEA 50151/C. Kennel
   1   SEA 31241/P. Chatterton
   1   SEA 03R/L. Benen
   1   SEA 03R/R. Dilts
   1   SEA 03R/N. Kobitz
   1   SEA 03R/J. Schuler
   1   SEA 05R24/J. Sejd
   1   SEA 50B/P.A. Gale
   1   SEA 3213/E.N. Comstock
   1   SEA 321/R.G. Keane, Jr.
   1   SEA 3213/W. Livingston
   1   SEA 61433/F. Prout

12   DTIC

1   NSF/Engineering Lib

1   DOT/Lib TAD-491.1

1   NBS/Klebanoff

1   MARAD/Lib

Copies

5   U. of Cal./Dept Naval Arch, Berkeley
   1   Eng Library
   1   Webster
   1   Paulling
   1   Wehausen
   1   Yeung

2   U. of Cal., San Diego
   1   A.T. Ellis
   1   Scripps Inst Lib

2   CIT
   1   Aero Lib
   1   T.Y. Wu

1   Catholic U. of Amer/Civil & Mech Eng

1   Colorado State U./Eng Res Cen

1   Florida Atlantic U.
   1   Tech Lib

1   U. of Hawaii/St. Denis

1   U. of Illinois/J. Robertson

2   U. of Iowa
   1   Library
   1   Landweber

1   U. of Kansas/Civil Eng Lib

1   Lehigh U./Fritz Eng Lab Lib

3   MIT
   1   Ogilvie
   1   Abkowitz
   1   Newman

2   U. of Mich/NAME
   1   Library
   1   M. Parsons

1   U. of Notre Dame
   1   Eng Lib

Copies			Copies		
2	New York U./Courant Inst		1	Maritime Research Information Service	
	1	A. Peters			
	1	J. Stoker			

Copies		
4	SIT	
	1	Breslin
	1	Savitsky
	1	Dalzell
	1	Kim

CENTER DISTRIBUTION

Copies	Code	Name
1	1500	W.B. Morgan
1	1504	V.J. Monacella
1	1520	W.C. Lin
1	1521	W.G. Day
1	1521	A.M. Reed
1	1522	G.F. Dobay
1	1522	M.B. Wilson
1	1522	Y.H. Kim
1	1540	J.H. McCarthy
1	1540	B. Yim
1	1542	Branch Head
1	1542	F. Noblesse
1	1560	D. Cieslowski
1	1561	G.C. Cox
1	1561	S.L. Bales
1	1561	W.R. McCreight
1	1561	J.F. O'Dea
1	1562	D.D. Moran
1	1562	E.E. Zarnick
1	1562	K.K. McCreight
10	1562	Y.S. Hong
1	1563	D.T. Milne
1	1564	J.P. Feldman
1	1564	R.M. Curphey
30	5211.1	Reports Distribution
1	522.1	Unclassified Lib (C)
1	522.2	Unclassified Lib (A)

Left column continued:

Copies		
1	U. of Texas/Arl Lib	
2	Southwest Res Inst	
	1	Applied Mech Rev
	1	Abramson
1	Stanford Res Inst/Lib	
2	U. of Washington	
	1	Eng Lib
	1	Mech Eng/Adee
3	Webb Inst	
	1	Library
	1	Lewis
	1	Ward
1	Woods Hole/Ocean Eng	
1	SNAME/Tech Lib	
1	Bethlehem Steel/New York/Lib	
1	General Dynamics, EB/Boatwright	
1	Gibbs & Cox/Tech Info	
1	Hydronautics	
	1	Library
1	Newport News Shipbuilding/Lib	
1	Sperry Rand/Tech Lib	
1	Sun Shipbuilding/Chief Naval Arch	
2	American Bureau of Shipping	
	1	Lib
	1	Cheng

END

FILMED

11-83

DTIC